

OPEN

# (–)-Epigallocatechin gallate inhibits stemness and tumourigenicity stimulated by AXL receptor tyrosine kinase in human lung cancer cells

Kozue Namiki<sup>1,2,5</sup>, Pattama Wongsirisin<sup>1,2,5</sup>, Shota Yokoyama<sup>1,2</sup>, Motoi Sato<sup>1,2</sup>, Anchalee Rawangkan<sup>1,2,3</sup>, Ryo Sakai<sup>1,2</sup>, Keisuke Iida<sup>1,2,4</sup> & Masami Suganuma<sup>1,2\*</sup>

Cancer stem cells (H1299-sdCSCs) were obtained from tumour spheres of H1299 human lung cancer cells. We studied low stiffness, a unique biophysical property of cancer cells, in H1299-sdCSCs and parental H1299. Atomic force microscopy revealed an average Young's modulus value of 1.52 kPa for H1299-sdCSCs, which showed low stiffness compared with that of H1299 cells, with a Young's modulus value of 2.24 kPa. (–)-Epigallocatechin gallate (EGCG) reversed the average Young's modulus value of H1299-sdCSCs to that of H1299 cells. EGCG treatment inhibited tumour sphere formation and *ALDH1A1* and *SNAI2* (*Slug*) expression. AXL receptor tyrosine kinase is highly expressed in H1299-sdCSCs and AXL knockdown with siAXLs significantly reduced tumour sphere formation and *ALDH1A1* and *SNAI2* (*Slug*) expression. An AXL-high population of H1299-sdCSCs was similarly reduced by treatment with EGCG and siAXLs. Transplantation of an AXL-high clone isolated from H1299 cells into SCID/Beige mice induced faster development of bigger tumour than bulk H1299 cells, whereas transplantation of the AXL-low clone yielded no tumours. Oral administration of EGCG and green tea extract (GTE) inhibited tumour growth in mice and reduced p-AXL, *ALDH1A1*, and *SLUG* in tumours. Thus, EGCG inhibits the stemness and tumourigenicity of human lung cancer cells by inhibiting AXL.

Green tea and (–)-epigallocatechin gallate (EGCG), the main constituent of green tea catechins, prevent cancer in humans, as demonstrated in phase II clinical trials, which showed that EGCG prevented colorectal adenoma recurrence and prostate cancer development from high-grade prostate intraepithelial neoplasia<sup>1–4</sup>. Numerous investigators have reported therapeutic effects in various human cancer cell lines by combining EGCG and other green tea catechins with anticancer compounds, including anticancer drugs, nonsteroidal anti-inflammatory drugs, and phytochemicals<sup>5,6</sup>. Because EGCG inhibits the expression of stemness marker genes and epithelial–mesenchymal transition (EMT)-related genes in human cancer stem cells (CSCs) of the breast, lung, prostate and liver, CSCs are targets of EGCG for cancer prevention and therapy<sup>7</sup>.

Using atomic force microscopy (AFM), Gimzewski's laboratory first reported that metastatic cancer cells obtained from the pleural fluids of various cancer patients showed lower average Young's modulus values, indicating lower cell stiffness, than those of normal mesothelial cells from pleural effusion<sup>8</sup>. Furthermore, they showed that treatment with green tea extract (GTE) increased the average Young's modulus values for metastatic cancer cells (i.e., reversed the values to those of normal cell stiffness levels)<sup>9</sup>. Our previous study revealed that EGCG increased the stiffness of H1299 and Lu99 human non-small cell lung cancer (NSCLC) cells, inhibited the high expression of EMT-related proteins, such as vimentin and *SLUG*, and reduced cell motility<sup>10</sup>. To investigate the inhibitory effects of EGCG on the biophysical properties of CSCs, we enriched CSCs from the tumour spheres of

<sup>1</sup>Graduate School of Science and Engineering, Saitama University, Saitama, 338-8570, Japan. <sup>2</sup>Research Institute for Clinical Oncology, Saitama Cancer Center, Saitama, 362-0806, Japan. <sup>3</sup>School of Medical Science, University of Phayao, Phayao, Thailand, 56000. <sup>4</sup>Molecular Chirality Research Center and Department of Chemistry, Graduate School of Science, Chiba University, Chiba, 263-8522, Japan. <sup>5</sup>These authors contributed equally: Kozue Namiki and Pattama Wongsirisin. \*email: [masami0306@mail.saitama-u.ac.jp](mailto:masami0306@mail.saitama-u.ac.jp)

H1299 cells (H1299-sdCSCs). H1299-sdCSCs overexpressed both stemness marker genes (*CD133*, *ALDH1A1*, *NANOG*, *SOX2*, and *OCT4*) and EMT-related genes (*CDH2* (*N-cadherin*), *VIM* (*Vimentin*), *SNAI1* (*Snail*), *SNAI2* (*Slug*), and *ZEB1*). We aimed to characterize the critical factors regulating the biophysical and stemness properties of H1299-sdCSCs and identify targets for preventing cancer with EGCG.

We recently reported that AXL receptor tyrosine kinase (AXL) stimulates cell softening and motility in H1299 and Lu99 human lung cancer cells<sup>11</sup>. AXL was isolated as a novel transforming gene from patients with chronic myelogenous leukemia; the name ‘AXL’ was derived from the Greek word for ‘non-controlled’<sup>12,13</sup>. The AXL protein belongs to the TAM (TYRO3, AXL, and MER) receptor tyrosine kinase family and is activated by growth arrest-specific 6 (GAS6), resulting in autophosphorylation of the Y702 and Y703 residues<sup>14</sup>. High coexpression of AXL and GAS6 is a risk factor for poor survival in lung cancer patients<sup>15</sup>. AXL has attracted attention as a driver of therapeutic resistance, i.e., high AXL expression is closely associated with the acquisition of drug resistance in lung and breast cancer cells<sup>16,17</sup>. Furthermore, AXL stimulates the self-renewal of stem cells from breast cancer, chronic myelogenous leukaemia, and glioblastoma<sup>18–20</sup>. Our experiments showed that a human NSCLC cell line, H1299, expressed high amounts of both AXL and phosphorylated AXL (p-AXL, an active form) and revealed that treating H1299 cells with AXL-targeted siRNA increased the average Young’s modulus value. These findings indicated that the stiffness of the H1299 cells was reversed and that motility was inhibited to the levels of the low-motile high-stiffness H1703 NSCLC cell line, as if the cells had been treated with EGCG<sup>11</sup>. Thus, AXL appears to play a significant role in the stemness of H1299-sdCSCs.

We revealed that H1299-sdCSCs possessed less stiffness and softer elasticity than the H1299-parental cells, and EGCG reversed the lower stiffness of the H1299-sdCSCs to the same stiffness of the H1299-parental cells, suggesting that AXL expression was inhibited in the H1299-sdCSCs. Treatment with EGCG and siAXL similarly induced the following inhibitory effects on the H1299-sdCSCs: 1) a reduction in tumour sphere formation; 2) inhibition of *ALDH1A1* and *SNAI2* (*Slug*) but not other stemness markers or EMT-related genes; and 3) a reduction in aldehyde dehydrogenase (ALDH)-positive cells. Furthermore, high AXL and p-AXL levels in the AXL-high clone strongly induced the tumorigenicity of H1299 cells in SCID/Beige mice, and oral administration of EGCG + GTE inhibited the tumour growth of H1299 cells by reducing p-AXL, SLUG and ALDH1A1 levels. The results suggest that AXL contributes to the stemness of H1299-sdCSCs and is a unique target for cancer prevention with EGCG.

## Results

**Inhibitory effects of green tea catechins on the tumour sphere formation of H1299 cells.** We first confirmed that H1299 human lung cancer cells produced  $35.0 \pm 8.7$  tumour spheres under non-attached and serum-free culture conditions. To determine the stemness properties, tumour spheres were first separated from parental H1299 cells using a filter with a pore size of more than  $77 \mu\text{m}$ . Since the cells of the tumour spheres differed qualitatively from the parental H1299 cells, we named the cells H1299-sdCSC. H1299-sdCSCs had significantly increased expression of the stemness marker genes, *CD133* (2.2-fold), *ALDH1A1* (69.9-fold), *NANOG* (8.5-fold), *SOX2* (19.2-fold), and *OCT4* (5.0-fold), and the EMT-related genes, *CDH2* (*N-cadherin*) (6.0-fold), *VIM* (*Vimentin*) (1.4-fold), *SNAI1* (*Snail*) (4.7-fold), *SNAI2* (*Slug*) (19.3-fold), and *ZEB1* (6.4-fold), compared with the parental H1299 (Supplementary Fig. S1).

EGCG induces anticancer activity by inhibiting the expression of stemness marker genes and self-renewal of human CSCs<sup>7</sup>. Green tea contains at least four green tea catechins, which are divided into two groups: the cancer preventive group, which includes EGCG, (–)-epigallocatechin (EGC), and (–)-epicatechin gallate (ECG); and the inactive group, which includes (–)-epicatechin (EC)<sup>21</sup>. The inhibitory effects of green tea catechins on H1299-sdCSCs were investigated in a tumour sphere formation assay, using two concentrations (10 and  $50 \mu\text{M}$ ) of each catechin. Treatment with  $50 \mu\text{M}$  EGCG,  $50 \mu\text{M}$  EGC, and  $50 \mu\text{M}$  ECG reduced the numbers of tumour spheres from  $35.0 \pm 8.7$  to  $16.0 \pm 3.5$ ,  $27.6 \pm 5.5$ , and  $23.7 \pm 2.1$ , respectively. Compared with the control, tumour sphere formation was reduced by 51.9%, 21.1%, and 30.7%, respectively. EC did not reduce tumour sphere formation (Fig. 1A). Among the catechins, EGCG inhibited tumour sphere formation most effectively, and previous results support that EGCG is the most active cancer preventive compound<sup>4</sup>. Tumour spheres treated with EGCG were smaller than non-treated cells (Fig. 1B). Importantly, EGCG significantly inhibited the proliferation of H1299-sdCSCs. The effects of EGCG and EC were also confirmed in another NSCLC cell line, Lu99, as shown in Supplementary Fig. S2.

**Biophysical properties of H1299-sdCSCs and their inhibition by EGCG.** We previously reported the results obtained by AFM that the highly metastatic mouse melanoma variant, B16-F10, had the lowest average Young’s modulus value among all melanoma variants tested<sup>21,22</sup>. Thus, we believe that cell stiffness, a biophysical phenotype of cancer, is a suitable indicator of metastatic potential. To measure cell stiffness, the trypsinized H1299-sdCSCs and H1299 cells were attached to biocompatible anchor for membrane (BAM)-coated dishes<sup>23</sup>. AFM measurement revealed that the average Young’s modulus values were  $2.24 \pm 0.07$  kPa for H1299 and  $1.52 \pm 0.03$  kPa for H1299-sdCSCs (Fig. 1C). This indicated that H1299-sdCSCs possessed less stiffness and softer elasticity than H1299. Furthermore, treatment with  $10 \mu\text{M}$  and  $50 \mu\text{M}$  EGCG increased the average Young’s modulus values of H1299-sdCSCs from  $1.52 \pm 0.03$  kPa to  $1.82 \pm 0.05$  kPa and  $2.04 \pm 0.05$  kPa, respectively (Fig. 1C). During AFM measurement, we observed that EGCG-treated H1299-sdCSCs showed a similar adherent phenotype to H1299-parental, and that suspended H1299 cells quickly adhered to BAM-coated dishes, but H1299-sdCSCs did not. We assumed that EGCG reversed the biophysical property of H1299-sdCSCs to that of H1299-parental cells, which was supported by our previous results that EGCG increased the stiffness of adhered cells in parental H1299<sup>10</sup>.

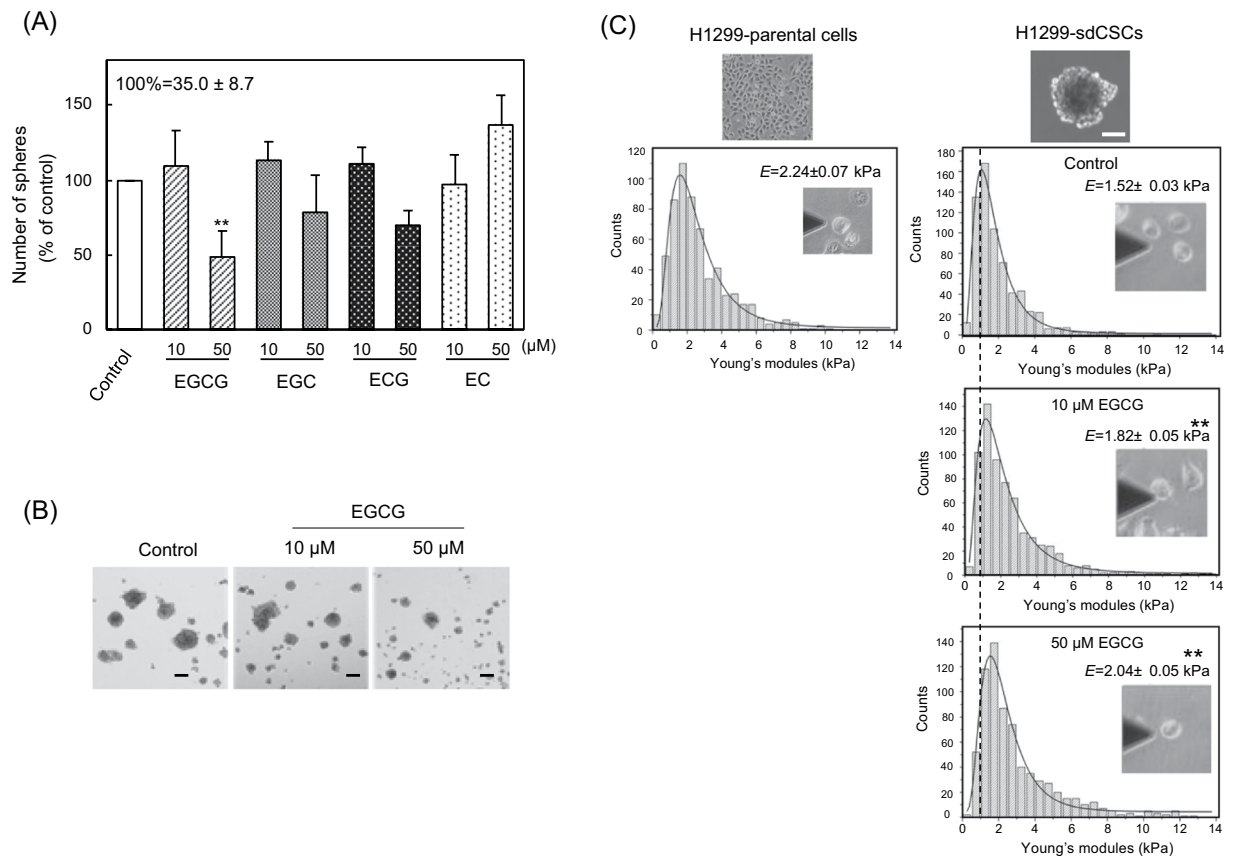


**Figure 1.** EGCG inhibited tumour sphere formation and increased stiffness of H1299-sdCSCs. **(A)** H1299 cells were cultured in serum-free medium in the presence of 10 μM or 50 μM green tea catechins, including EGCG, EGC, ECG, and EC, for 3 weeks. The results are expressed as the mean % of the control ± SD from three independent experiments. **(B)** Representative images of tumour spheres treated with vehicle and EGCG. Black bars indicate 100 μm. **(C)** Histogram of average Young's modulus values for cells separated from H1299-sdCSCs compared with those from H1299-parental cells. Separated cells from H1299-sdCSCs were attached to a BAM-coated dish, then measured via AFM. The black line indicates the lognormal fitting curve for each treatment, and the dotted line indicates the average Young's modulus value of the control H1299-sdCSCs.  $E$  values indicate the average Young's modulus value ± SD from three independent experiments. \*\* $P < 0.01$ , \* $P < 0.05$ .

### Inhibition of *ALDH1A1* and *SNAI2 (Slug)* expression in H1299-sdCSCs treated with EGCG was associated with reduced ALDH-positive cells.

The inhibitory effects of EGCG on the expression of five stemness marker genes and five EMT-related genes in H1299-sdCSCs were studied. Treatment with 10 μM EGCG reduced *ALDH1A1* expression to  $0.23 \pm 0.12$ , and treatment with 50 μM EGCG reduced *SNAI2 (Slug)* expression to  $0.20 \pm 0.12$  compared with that of H1299-sdCSCs without EGCG (Table 1). However, EGCG did not change the expression of other stemness marker genes (*CD133*, *NANOG*, *SOX2*, and *OCT4*) or other EMT-related genes (*CDH2 (N-cadherin)*, *VIM (vimentin)*, *SNAI1 (Snail)*, and *ZEB1*) (Table 1). Other investigators similarly reported that ALDH is highly expressed in spheroid-derived CSCs of human colorectal cancer (HCT116-SDCSCs) compared with that in parental cells, and that ALDH activity is associated with *ALDH1A1* expression and high tumorigenicity<sup>24,25</sup>. The percentage of ALDH-positive cells in both H1299 and H1299-sdCSCs was determined by Aldefluor flow cytometry, and we found that the proportion of ALDH-positive cells in H1299-sdCSCs were approximately 3- to 5-fold more than that in H1299 cells (Fig. 2A). In addition, treatment with 10 μM and 50 μM EGCG dose-dependently decreased the percentages of ALDH-positive cells in H1299-sdCSCs by approximately 0.6- and 0.4-fold, respectively (Fig. 2A). We confirmed that EGCG reduced ALDH1A1 protein levels in H1299-sdCSCs by immunocytochemical analysis (Fig. 2B). The results suggest that ALDH and SLUG in H1299-sdCSCs contributed to stemness, which was inhibited by EGCG.

**EGCG inhibited AXL expression in H1299-sdCSCs.** AXL is a receptor tyrosine kinase. We previously reported that AXL stimulates H1299 cell softening, and treatment with the R428 AXL inhibitor reversed it<sup>11</sup>. As aforementioned, H1299 cells contain both high amounts of AXL protein and p-AXL at Y702. H1299 treated with 50 μM EGCG and 50 μM EGC had reduced p-AXL/AXL ratios of 0.58 and 0.64, respectively (Supplementary Fig. S3), suggesting that green tea catechins inhibited AXL activation.

We next studied the relationship between stemness and AXL protein expression in EGCG-treated H1299sd-CSCs. Flow cytometric analysis using anti-AXL antibody and AF647-labeled secondary antibody revealed that H1299-sdCSCs consisted of two populations with different AXL protein expression levels on the

	Relative expression (fold of the control) <sup>†</sup>				
	EGCG (10 μM)	EGCG (50 μM)	siControl	siAXL-1	siAXL-2
<b>Stemness genes</b>					
<i>CD133</i>	1.07 ± 0.33	1.44 ± 0.01	1.64 ± 0.69	5.64 ± 0.83	1.70 ± 0.46
<i>Nanog</i>	1.05 ± 0.47	1.11 ± 0.47	1.14 ± 0.65	2.30 ± 1.24	1.35 ± 0.60
<i>Sox2</i>	0.70 ± 0.32	0.96 ± 0.08	1.32 ± 0.37	1.42 ± 0.65	2.08 ± 1.09
<i>Oct4</i>	1.01 ± 0.56	1.11 ± 0.39	1.12 ± 0.37	1.92 ± 1.16	1.25 ± 0.52
<i>ALDH1A1</i>	<u>0.23 ± 0.12*</u>	1.53 ± 1.32	1.23 ± 0.41	0.78 ± 0.87	<u>0.31 ± 0.20*</u>
<b>EMT-marker genes</b>					
<i>CDH2 (N-Cadherin)</i>	1.26 ± 1.08	0.99 ± 0.46	2.23 ± 0.06	2.33 ± 0.89	2.03 ± 1.13
<i>VIM (Vimentin)</i>	1.00 ± 0.36	1.09 ± 0.27	1.07 ± 0.22	1.00 ± 0.04	1.03 ± 0.26
<i>SNAI1 (Snail)</i>	1.14 ± 0.24	1.47 ± 0.29	1.05 ± 0.09	0.90 ± 0.41	0.87 ± 0.23
<i>SNAI2 (Slug)</i>	0.68 ± 0.18	<u>0.20 ± 0.12*</u>	1.42 ± 0.58	<u>0.41 ± 0.24**</u>	<u>0.38 ± 0.19**</u>
<i>ZEB1</i>	1.24 ± 0.25	1.09 ± 0.09	1.32 ± 0.21	1.25 ± 0.14	1.25 ± 0.30

**Table 1.** Specific inhibition of *ALDH1A1* and *SNAI2 (Slug)* gene expressions in H1299-sdCSCs after treatment with EGCG and siAXL. <sup>†</sup>Expression level of each gene normalized by GAPDH in control H1299-sdCSCs expressed as 1.0. \**P* < 0.05, \*\**P* < 0.01.

membrane: 38.8% for the high AXL-expressing population (AXL-high) and 61.2% for the low AXL-expressing population (AXL-low) (Fig. 2C). Treatment with 10 μM and 30 μM EGCG reduced the percentage of the AXL-high population from 38.8% to 30.0% and 19.9%, respectively, and decreased the mean fluorescence intensity (MFI) of the AXL protein from 2,199 ± 100 to 1,655 ± 32 and 1,585 ± 277 (Fig. 2C), respectively, indicating that EGCG inhibited AXL protein expression in H1299-sdCSCs.

**Contribution of AXL to H1299-sdCSC stemness.** GAS6, a protein related to the anticoagulation factor protein S, is a ligand for the AXL and TAM family of receptor tyrosine kinases<sup>14</sup>. To study the contribution of AXL activation to H1299-sdCSC stemness, the effect of GAS6 on tumour sphere formation was examined. Treatment of H1299 cells with GAS6 at 250 ng/ml increased p-AXL protein levels by approximately 8-fold, suggesting that GAS6 induced AXL activation (Fig. 3A). GAS6 treatment in the tumour sphere assay induced significantly larger spheres than those from cells without GAS6 and increased the number of tumour spheres from 100% (38.3 ± 6.5) to 146% (56.0 ± 9.5; Fig. 3A). Importantly, activating AXL with GAS6 stimulated tumour sphere formation and stemness.

We next transfected siAXL-1 and siAXL-2 into H1299 cells to reduce AXL protein levels (Fig. 3B). Treatment with siAXL-1 and siAXL-2 reduced the numbers of tumour spheres to 13.3% (5.3 ± 1.5) and 20.8% (8.3 ± 3.5) in the non-treated H1299 (40.0 ± 8.9), respectively, and the inhibitory effect with siAXLs was more effective than 44.3% (17.7 ± 4.0) with the siControl (Fig. 3B). Consistent with evidence showing that EGCG reduces *ALDH1A1* and *SNAI2 (Slug)* expression, treatment with siAXL-1 and siAXL-2 also reduced *ALDH1A1* (0.78 and 0.31) and *SNAI2 (Slug)* (0.41 and 0.38) expression among five stemness marker genes and five EMT-related genes in H1299-sdCSCs (Table 1). Furthermore, H1299-sdCSCs treated with two siAXLs had a reduced percentage of ALDH-positive cells, as detected by flow cytometry, and reduced *ALDH1A1* protein levels, as determined by immunocytochemistry, compared with non-treated H1299-sdCSCs (Fig. 3C,D). The contribution of AXL to CSCs was also confirmed in Lu99 cells and H1703-AXL cells: treatment with siAXL-1 and siAXL-2 significantly reduced the proportions of tumour spheres to 61.1% and 21.2%, respectively, in Lu99 cells (Supplementary Fig. S4). Furthermore, exogenous AXL expression stimulated tumour sphere formation in H1703 cells, which express AXL at lower levels than H1299 cells (Supplementary Fig. S5). These results suggest that AXL protein stimulates *ALDH1A1* and *SNAI2 (Slug)* expression, and increases ALDH protein and ALDH activity, suggesting that AXL is related to tumour sphere formation and stemness.

**Enhanced tumourigenicity of AXL-high clones and absent tumourigenicity of AXL-low clones.** To characterize the role of AXL in tumourigenicity, we sorted 15% of the H1299 cells as the AXL-high population and 15% as the AXL-low population by flow cytometry (Fig. 4A), and then established two cell clones: an AXL-high clone with high levels of both p-AXL and AXL, and an AXL-low clone with lower levels of both proteins. The p-AXL/AXL ratios were 7.0–13.2 and zero for the AXL-high and AXL-low clones, respectively, and the AXL/α-tubulin ratios were 1.9–2.7 and 0.5–0.7 for the AXL-high and AXL-low clones, respectively, compared with those of the bulk H1299 cells (Fig. 4B).

The same amounts (1 × 10<sup>6</sup> cells) of the two clones and the bulk H1299 cells as a control were subcutaneously transplanted into SCID/Beige mice. The AXL-high clone produced larger tumours more rapidly than the bulk H1299 cells, whereas the AXL-low clone developed no tumours at 12 injection sites in six mice by day 35 of the experiment. Importantly, all the AXL-high clones had produced tumours by day 31 (Fig. 4C). Tumours derived from the AXL-high clone contained high levels of p-AXL and AXL compared with those from the H1299 cells (Fig. 4D). These results indicated that p-AXL and AXL proteins are important for high tumourigenicity.

**EGCG inhibited the tumour growth of H1299 cells by reducing p-AXL, *ALDH1A1*, and *SLUG*.** Since p-AXL is an essential factor for stemness, we examined the inhibitory effect of EGCG on tumour growth in

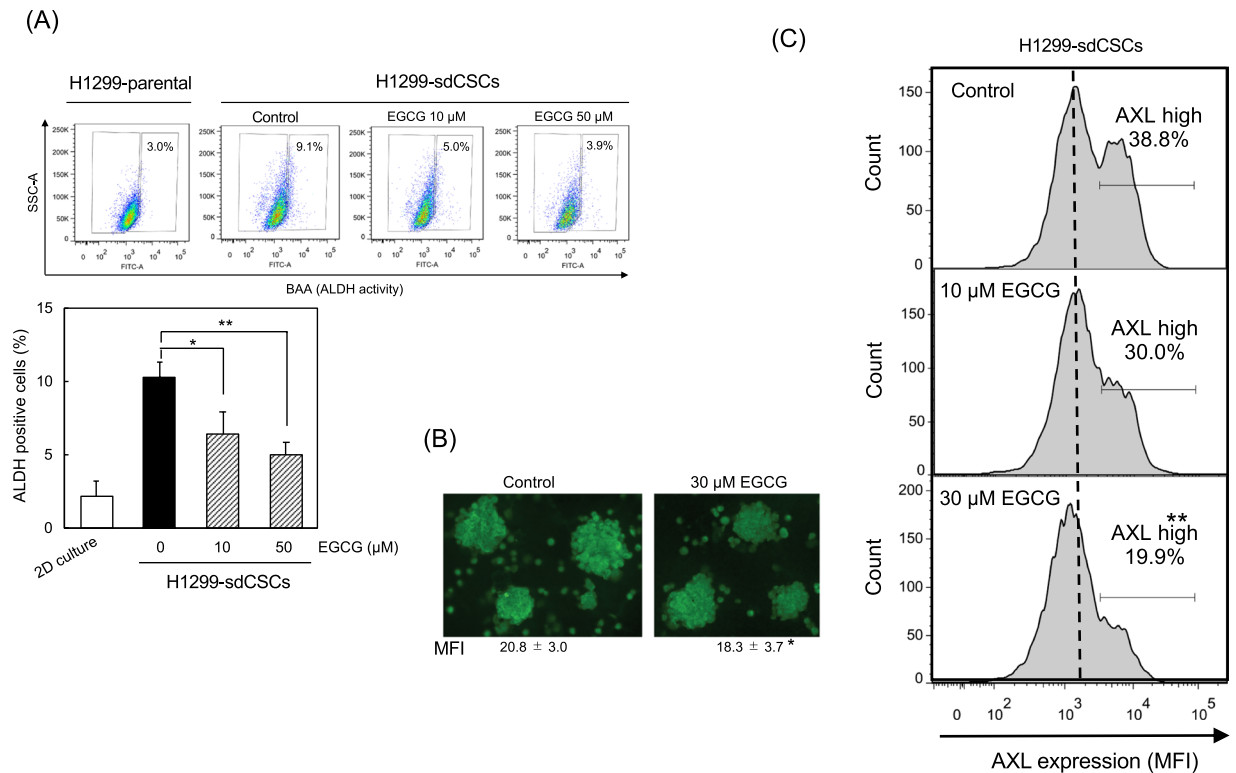


**Figure 2.** Reduced ALDH-positive cells, ALDH levels, and AXL levels in H1299-sdCSCs. **(A)** Average percentage of ALDH-positive cells in H1299-sdCSCs. The upper figure shows representative results detected by Aldefluor flow cytometry assay in H1299-parental cells and H1299-sdCSCs treated with vehicle (Control), 10  $\mu$ M, and 50  $\mu$ M EGCG. Baseline fluorescence was established by inhibiting ALDH activity with DEAB. The lower graph shows the mean  $\pm$  SD of the percentage of ALDH-positive cells from three independent experiments. **(B)** Representative images of immunocytochemical staining of ALDH1A1 in non-treated and 30  $\mu$ M EGCG-treated H1299-sdCSCs. Numbers indicate the mean fluorescence intensity (MFI) of 15 tumour spheres from three independent experiments. **(C)** AXL protein levels in the H1299-sdCSCs were examined via flow cytometry using anti-AXL antibody and AlexaFluor 647-labeled secondary antibody. The dotted line indicates MFI in the control H1299-sdCSCs. Three independent experiments were conducted. \*\* $P < 0.01$ , \* $P < 0.05$ .

H1299 cells *in vivo* using a mouse xenograft model. EGCG (100 mg/kg) and 0.2% GTE were administered from one day before injection of H1299 ( $10^6$  cells/injection) to the end of the experiment. The total amount of green tea catechins per day/mouse was estimated as 4.4 mg/mouse, the equivalent of 10 cups of green tea/day, which is the cancer preventive amount for humans<sup>1–4</sup>. The group treated with EGCG + GTE showed delayed tumour development (Fig. 5A); tumours were found in 75% (9/12) of the injected sites of the EGCG + GTE group, whereas tumours of the non-treated group developed in 100% (12/12) of the injected sites at 35 days after injection (Fig. 5B). The tumour size of the EGCG + GTE group was relatively smaller than that of the non-treated group (Fig. 5B), and the average tumour weight of the EGCG + GTE group was  $0.05 \pm 0.06$  g, which was significantly lower than that of the non-treated group ( $0.10 \pm 0.06$  g; Fig. 5C). Notably, tumours of the EGCG + GTE group had lower levels of p-AXL and AXL compared with those of the non-treated group. In addition, EGCG + GTE inhibited AXL activation in tumours (Fig. 5D), which possessed lower levels of ALDH1A1 and SLUG proteins than those of the non-treated group (Fig. 5D). The p-AXL levels were well correlated with the ALDH1A1 and SLUG levels in the tumours, with *r* values of 0.87 and 0.65 (Fig. 5E). Thus, we concluded that the ALDH1A1 and SLUG axis regulated by AXL is involved in tumourigenicity and stemness, and that cancer prevention with EGCG mediates inhibition of the AXL/ALDH/SLUG axis.

## Discussion

Here we report for the first time the biophysical properties of H1299-sdCSC human lung cancer stem cells. AFM revealed that the average Young's modulus value for H1299-sdCSCs was 1.52 kPa, which was 0.68-fold lower than that for the parental H1299 at 2.24 kPa. A previous investigation using AFM reported a 0.7-fold lower stiffness in a human hepatoma stem cell line, MHCC97H, compared with that of the parental cells<sup>26</sup>. Other researchers using a microfluidic device reported a higher deformability in ALDH<sup>+</sup> CSCs isolated from an inflammatory breast cancer cell line, SUM149, than that in ALDH<sup>-</sup> cells<sup>27</sup>. Cross *et al.* first reported that the average Young's modulus value for metastatic cancer cells isolated from the pleural fluid of lung, breast, and pancreatic cancer patients tended to be approximately 0.33-fold lower than that of normal mesothelial cells<sup>8</sup>. We think that low stiffness, soft elasticity, high deformability, and metastatic potential are unique biophysical properties of CSCs isolated

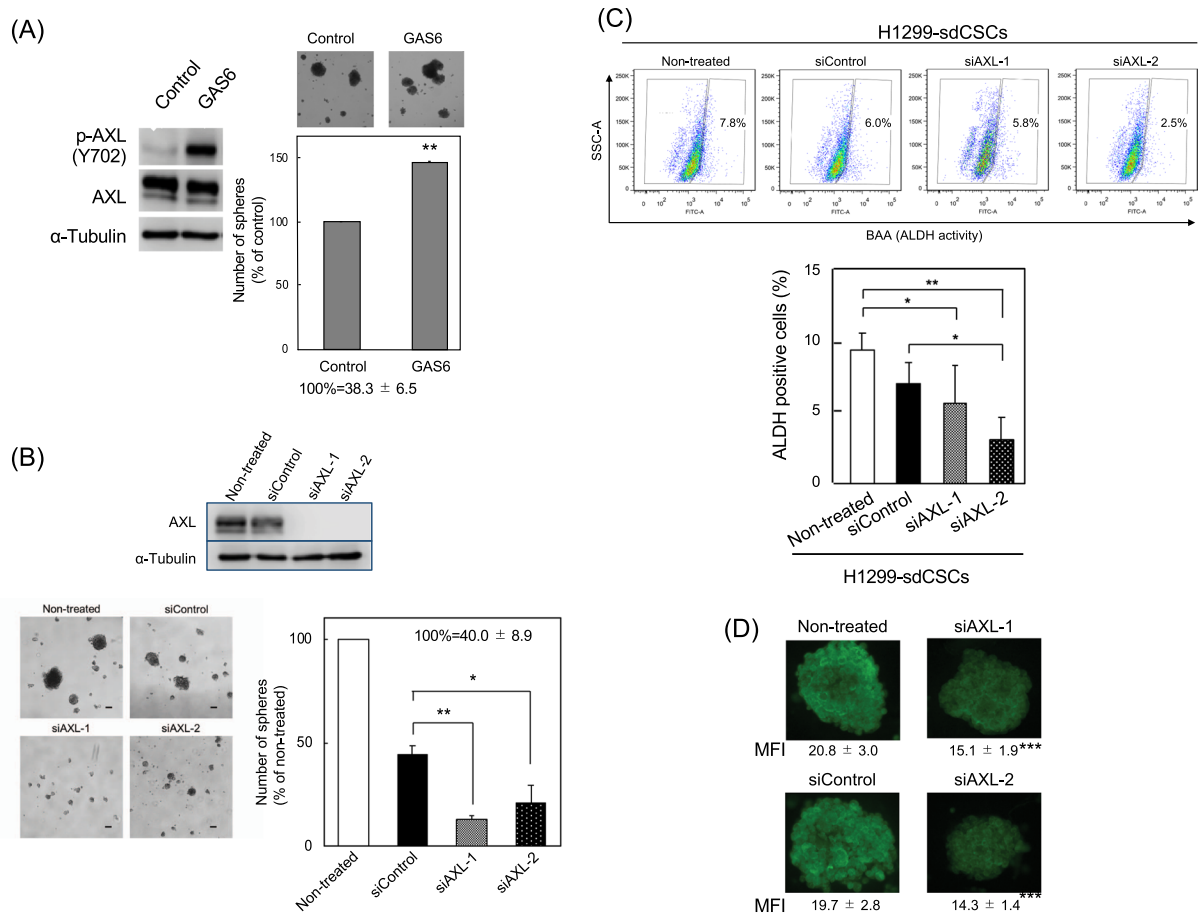


**Figure 3.** Involvement of AXL in tumour sphere formation and ALDH activity in H1299-sdCSCs. **(A)** Treatment of H1299-sdCSCs with GAS6 (250 ng/ml) significantly increased phosphorylated AXL (p-AXL Y702) (p-AXL/AXL) compared with that in control cells, as analysed by western blotting.  $\alpha$ -Tubulin was used as a control. This blot is a part of Supplementary Fig. S2B. Tumour sphere formation was stimulated by treatment with GAS6 (100 ng/ml) for 3 weeks. The number of tumour spheres is shown as a percentage of the control. Three independent experiments were conducted. **(B)** Knockdown of AXL with siAXL-1 and siAXL-2 inhibited tumour sphere formation. Cells were treated with siAXLs or siControl for 2 days and then cultured in serum-free medium for 3 weeks. Images show representative tumour spheres. Percentages of tumour spheres of non-treated cells are shown in the graph. The results are the mean  $\pm$  SD of three independent experiments. **(C)** Knockdown of AXL with siAXL-1 and siAXL-2 reduced the percentage of ALDH-positive cells. ALDH-positive cells in H1299-sdCSCs treated with siControl, siAXL-1, or siAXL-2 were detected by Aldefluor flow cytometry assay. The upper figure shows the representative results. The graph shows the average percentage of ALDH-positive cells in three independent experiments. Full-length blots/gels are presented in Supplementary Information WB-1 and -2. **(D)** Representative images of ALDH1A1 immunocytochemical staining in non-treated, siControl-, siAXL-1-, and siAXL-2-treated H1299-sdCSCs. Numbers indicate MFI of 15 tumour spheres from three independent experiments. \* $P < 0.05$ , \*\* $P < 0.01$ , \*\*\* $P < 0.001$ .

from various human cancers and that an investigation of the biophysical properties of CSCs is needed to advance cancer research. The cancer preventive activity of EGCG was effectively found in stiffened cells and in the tumour sphere formation of H1299-sdCSCs. Sun *et al.* reported that salinomycin, one of the most potent anti-CSC compounds screened by Weinburg *et al.*, increases liver CSC stiffness in a manner similar to that of EGCG<sup>28,29</sup>.

OCT4, NANOG, and SOX2 are transcription factors that are required to maintain pluripotency<sup>30</sup>. Sphere-derived CSCs of colorectal cancer (HCT116-SDCSCs) express significantly higher levels of stemness marker genes, for example, 4.5-fold higher levels of OCT4 and 3.2-fold higher levels of NANOG compared with those of the parental cells<sup>25</sup>. We also found that H1299-sdCSCs expressed OCT4, NANOG, and SOX2 genes at levels of 5-fold more than the parental H1299 cells. Our study revealed that EGCG inhibited ALDH1A1 and SNAI2 (*Slug*) expression and ALDH activity, but not OCT4, NANOG, or SOX2 expression. Other investigators reported that EGCG inhibited the mRNA and protein expression of stemness markers, including OCT4 and NANOG, and increased the apoptotic markers BAX and caspase-8 in 20 human CSC lines collected from nine different cancer tissues<sup>7</sup>. But EGCG selectively inhibits ALDH and SLUG in this study. Some investigators reported that ALDH acts as a critical factor for cancer stemness<sup>31</sup>, and that SLUG promotes the expansion of CSCs in NSCLC by interacting with SOX9<sup>32</sup>. However, the mechanism of ALDH and SLUG has not yet been elucidated.

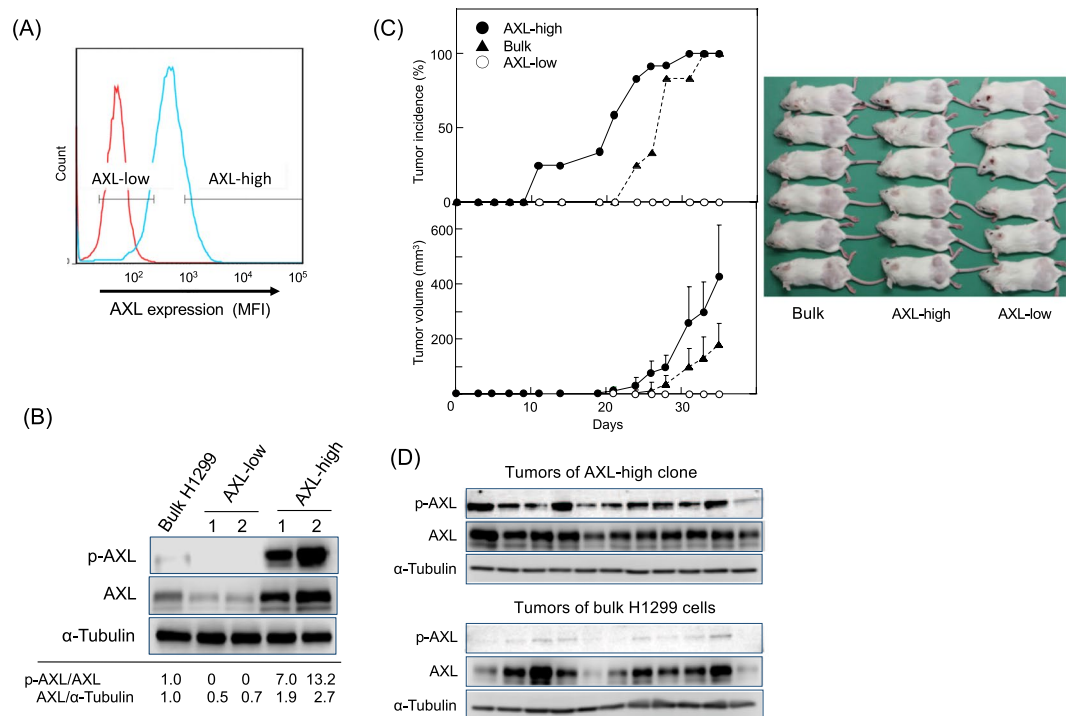


**Figure 4.** High tumorigenicity of AXL-high clone and no tumorigenicity of AXL-low clone. **(A)** AXL-high and AXL-low clones were isolated from 15% of the cells with the highest AXL expression and 15% of the cells with the lowest AXL expression, respectively, by flow cytometry using an anti-AXL antibody. **(B)** AXL and p-AXL levels in bulk H1299 cells, AXL-low, and AXL-high clones. Numbers indicate fold levels of p-AXL/AXL and AXL/ $\alpha$ -tubulin compared with those of bulk H1299 cells. Full-length blots/gels are presented in Supplementary Information WB-3. **(C)** Tumour incidences and tumour volume in the AXL-high clone ( $\bullet$ ), bulk H1299 cells ( $\blacktriangle$ ), and the AXL-low clone ( $\circ$ ). The same number of cells ( $1 \times 10^6$ ) were subcutaneously transplanted into the backs of SCID/Beige mice. Tumour volume was calculated as described in the Materials and Methods. The image shows the mice in all three groups at 35 days after transplantation. **(D)** p-AXL and AXL levels in tumours of AXL-high clone and bulk H1299 cells. p-AXL, AXL, and  $\alpha$ -tubulin (control) protein levels in tumours were examined by western blotting. Full-length blots/gels are presented in Supplementary Information WB-4. Tumour samples for western blotting were derived from the same experiment and gels/blots were generated in parallel and conducted three times.

AXL is reported to induce EMT and self-renewal in breast cancer cells and chronic myelogenous leukemia CSCs<sup>18,19</sup>, and has a crucial role in the CSCs of various cancers. Kinome-wide shRNA screening revealed AXL to be an upregulated and phosphorylated receptor tyrosine kinase (RTK) amongst 82 RTKs in mesenchymal glioma stem-like cells<sup>20</sup>. Highly phosphorylated AXL is often found in NSCLC tissues and cell lines, but AXL is not expressed in normal lung tissues. Flow cytometry analysis revealed the presence of two populations with different AXL protein levels in H1299-sdCSCs, and the AXL-high and AXL-low clones showed different tumorigenicities. Importantly, AXL-high clones contained 3.5–6.1-fold higher p-AXL protein levels than AXL-low clones, and the AXL-low clone did not contain p-AXL, indicating the essential contribution of p-AXL to tumorigenicity. Our results are well supported by evidence that the p-AXL levels in tumours of the EGCG + GTE group were strongly reduced by 0.36-fold compared with those of the non-treated group, whereas AXL levels in tumours from both groups were nearly the same. These results clearly indicate that tumorigenicity and stemness require AXL activation with high p-AXL levels.

AXL activation is both GAS6-dependent and -independent<sup>14</sup>. Because AXL interacts with cMET, EGF receptor (EGFR), and human EGFR-related 2 (HER2), AXL-RTK crosstalk induces the transactivation of AXL in lung and breast cancers<sup>16,33,34</sup>. AXL expression was positively associated with GAS6 expression, and high coexpression of AXL/GAS6 was a strong risk factor in one study population<sup>35</sup>. EGCG treatment reduced AXL phosphorylation in the absence and presence of GAS6 (Supplementary Fig. S3A,B), indicating that EGCG inhibits AXL activation in both a GAS6-dependent and -independent manner. We previously reported that EGCG altered membrane organization to rigid stiffness, which we termed the “sealing effect of EGCG”<sup>21</sup>. Matsuzaki *et al.* recently found that treatment with the giant liposome of EGCG increased the stiffened bending rigidity of the lipid membrane by approximately 60 times more than that without EGCG<sup>36</sup>. Because altering the membrane organization with EGCG inhibits EGFR activation, EGCG likely inhibits AXL transactivation via AXL/RTK crosstalk.

AXL acts as a driver for acquiring chemoresistance against tyrosine kinase inhibitors (TKIs) and conventional anticancer drugs. Zhang *et al.* reported that activating AXL caused resistance to EGFR-targeted TKIs such as erlotinib in lung cancer, and that genetic and pharmacological inhibition of AXL restored TKI sensitivity<sup>16</sup>. Therefore, AXL inhibitors are attracting attention to overcome chemosensitivity, and clinical studies of several specific AXL

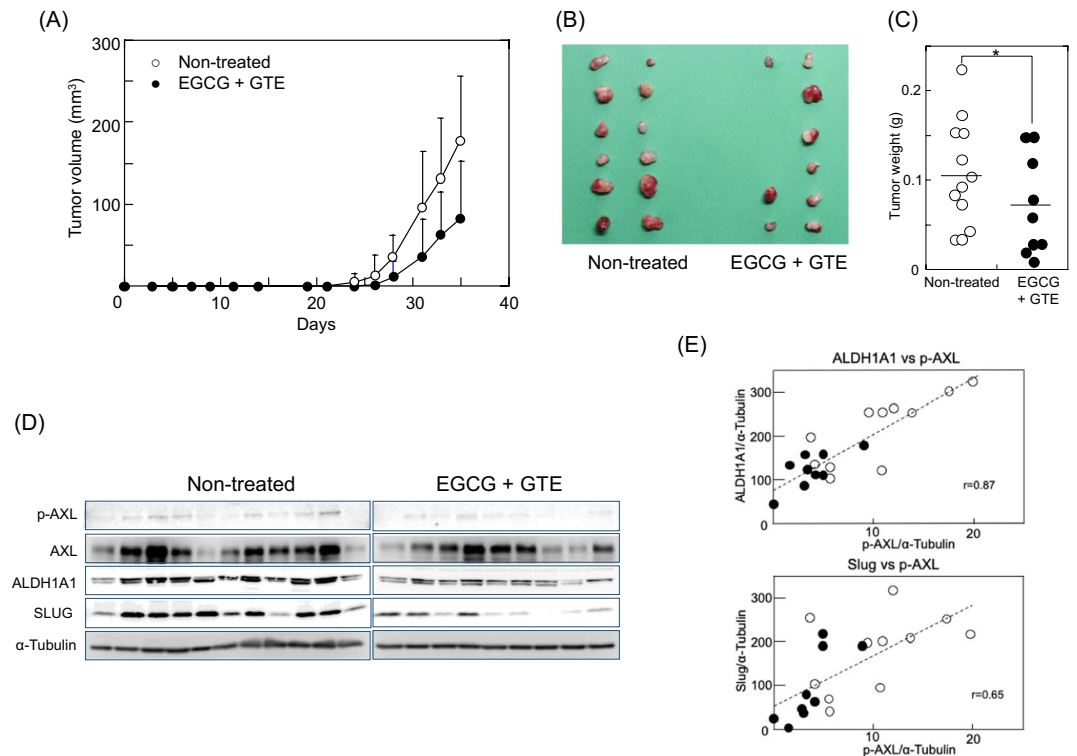


**Figure 5.** Oral administration of EGCG and GTE inhibited the tumour growth of H1299 cells by reducing p-AXL, ALDH1A1, and SLUG. **(A)** Tumour volume of the non-treated H1299 group (○) and the EGCG + GTE group (●). Mice in the EGCG + GTE group were given EGCG (100 mg/kg mice) via a gastric tube daily and 0.2% green tea extract as drinking water from one day before inoculating the cells. Tumour volume was calculated as described in the Materials and Methods. **(B)** The image shows all tumours that had developed in the two groups at 35 days post-transplantation. **(C)** Tumour weight of each tumour in the non-treated group (○) and in the EGCG + GTE group (●) \* $P < 0.05$ . **(D)** p-AXL, AXL, ALDH1A1, and SLUG protein levels in tumours were examined by western blotting.  $\alpha$ -Tubulin was used as a control. Two membranes were simultaneously measured for intensity via LAS 4000 IR for p-AXL, ALDH1A1, and SLUG levels. The blots for AXL, p-AXL, and  $\alpha$ -tubulin of the non-treated group are the same as those of the bulk H1299 cells group in Fig. 4D. Full-length blots/gels are presented in Supplementary Information WB-4. Tumour samples for western blotting were derived from the same experiment and gels/blots were generated in parallel and conducted three times. **(E)** Positive correlation between ALDH1A1 and p-AXL levels and between SLUG and p-AXL levels in tumours. Closed circles and open circles indicate those of each tumour in the EGCG-treated and non-treated groups, respectively. R values were 0.87 for ALDH1A1 vs. p-AXL and 0.65 for SLUG vs. p-AXL.

inhibitors are underway<sup>17</sup>. EGCG reversed cisplatin resistance by downregulating AXL and TYRO3 expression in NSCLC and sensitizing 5-FU-resistant colorectal cancer<sup>37</sup>. These results suggest that the combined effects of EGCG and other compounds inhibit stemness through the AXL axis.

Protein tyrosine phosphatase 4 A (PTP4A) is a member of the phosphatase of regenerating liver (PRL) family, and PRLs are oncogenic across many human cancers<sup>38</sup>. Here, we discussed the results of AXL activation; however, PTP4A in human cancers should be considered in future studies.

In conclusion, AXL regulates the biophysical properties of CSCs, including low stiffness and soft elasticity. Stiffening CSCs via AXL inhibition is a critical mechanism of the multiple benefits provided by EGCG, including preventing cancer, inhibiting metastasis, and overcoming chemoresistance.

## Methods

**Cell cultures and reagents.** The human NSCLC cell line, H1299 (ATCC CRL-5803), was purchased from American Type Culture Collection (ATCC; Manassas, VA, USA) and cultured in RPMI-1640 medium supplemented with 10% fetal bovine serum (Nichirei Bioscience Inc., Tokyo, Japan). The cells, which were confirmed as mycoplasma-free, were used at less than 20 passages and authenticated by short-tandem repeat profiling conducted by ATCC. EGCG of >98% purity was isolated from Japanese green tea leaves, and GTE was kindly provided by Dr. Atsuhiko Takahashi at Saitama Tea Institute, as described previously<sup>1,10</sup>. Anti-AXL (R&D Systems, Minneapolis, MN, USA), anti-p-AXL (Y702) (Cell Signaling Technology, Inc., Danvers, MA, USA), anti-SLUG (Cell Signaling Technology, Inc.), anti-ALDH1A1 (Santa Cruz, Biotechnology, Inc., Santa Cruz, CA, USA), and anti- $\alpha$ -tubulin (Cell Signaling Technology, Inc.) antibodies were used for the experiments.



**Tumour sphere formation.** H1299 cells were seeded at a density of 500 cells/well in serum-free medium (Dulbecco's modified Eagle's medium [DMEM]:F12 containing 0.45% methylcellulose, 50 ng/ml epidermal growth factor [EGF], 50 ng/ml fibroblast growth factor, and B27 supplement) in ultra-low-attachment 96-well plates (Corning Inc., Corning, NY, USA)<sup>39</sup>. Each treatment was conducted in six wells. After 3 weeks of culture, all wells were imaged using an All-in-One microscope (BZ-X700, Keyence, Tokyo, Japan), and the number of spheres measuring >100 µm on a minor axis were counted. Three independent experiments were conducted. Tumour spheres were separated from H1299-parental cells using a filter with a pore size of more than 77 µm (Spheroid Catch, Watson Co. Ltd, Tokyo, Japan) for gene expression analyses and AFM measurement.

**Cell stiffness measurement.** Tumour spheres were separated using 0.1% trypsin-0.02% EDTA solution, then seeded into 6-cm dishes (Thermo Fisher Scientific, Cambridge, MA, USA) coated with biocompatible anchor for membrane (BAM; NOF Corporation, Tokyo, Japan)<sup>23</sup>. After 1.5 h, 16 force-distance curves per cell were obtained via force-map analysis using AFM (MFP-3D-Bio-J-AFM, Asylum Research, CA, USA). Using the Hertz model, Young's moduli ( $E$ : kPa) were calculated from the force curves, as described previously<sup>22</sup>. Cell stiffness was obtained as the average Young's modulus value of 30 cells from a lognormal fitting curve.

**Knockdown of AXL with siRNA.** AXL-targeted siRNAs (s1845 and s1847, called siAXL-1 and siAXL-2, respectively) were purchased from Thermo Fisher Scientific. Supplementary Table S1 lists the siAXL sequences. A control siRNA (siControl) was obtained from OriGene Technologies, Inc. (Rockville, MD, USA). siRNA was transfected into H1299 cells using Lipofectamine RNAiMAX (Invitrogen, CA, USA) as described previously<sup>11</sup>. Cell stiffness, tumour sphere formation, and western blot analyses were conducted after 2 days.

**Western blot analysis.** Cells or tumours were lysed in strong lysis buffer containing 20 mM Tris-HCl at pH 8.0, 150 mM sodium chloride, 1% Triton X-100, 0.1% sodium dodecyl sulfate (SDS), 1% sodium deoxycholate, 10 µg/ml aprotinin, 10 µg/ml leupeptin, 1 mM phenylmethylsulfonyl fluoride, 1 mM sodium orthovanadate, 0.5 mM sodium pyrophosphate, and 5 mM sodium fluoride, as described previously<sup>11</sup>. The lysates were subjected to SDS-PAGE, and then transferred onto a nitrocellulose membrane. The membrane was then incubated with primary antibody overnight at 8 °C, then incubated with the appropriate horseradish peroxidase-conjugated secondary antibody against rabbit IgG or mouse IgG. Specific bands were then detected using ImmunoStar LD (Wako Pure Chem. Ind. Ltd., Tokyo, Japan) using the C-DiGit Chemiluminescent Western Blot Scanner (LI-COR Bioscience Inc., Lincoln, NE, USA) or the LAS 4000 IR multi-color (Fujifilm Co, Tokyo, Japan). Band intensity was measured using C-DiGit or ImageJ (National Institute of Health, Bethesda, MD, USA).  $\alpha$ -Tubulin was used as an internal control. At least three independent experiments were conducted.

**Quantitative real-time RT-PCR (qRT-PCR).** Total RNA isolated from the spheres was reverse transcribed into cDNA using oligo(dT)<sub>16</sub> and MuLV reverse transcriptase (Thermo Fisher Scientific), and real-time PCR was conducted using SYBR Green I (LightCycler 480, Roche Lifescience, Basel, Switzerland) as described previously<sup>40</sup>. The primers used are indicated in Supplementary Table S2. *GAPDH* was used as an internal control, and relative gene expression was calculated as the fold expression compared with that of the control tumour spheres or H1299-parental cells. At least three independent experiments were conducted.

**Flow cytometry analysis of AXL.** AXL protein level was examined via flow cytometry after incubation with anti-AXL antibody. Briefly, tumour spheres were treated with 0.1% trypsin and 0.02% EDTA solution containing 200 U/ml DNase I and 5 mM MgCl<sub>2</sub> for 3 min at 37 °C. Separated sphere-derived cells were incubated with anti-AXL antibody for 30 min on ice, washed, and further incubated with AlexaFluor647-conjugated anti-goat IgG antibody (Invitrogen, Waltham, MA, USA) for 30 min on ice. Fluorescence intensity was determined via flow cytometry (BD FACSCanto II, BD Bioscience, San Jose, CA, USA)<sup>40</sup>. The experiments were independently conducted three times. Fifteen percent of both the AXL-high and AXL-low populations from H1299 cells were sorted using the BD FACS AriaIII (BD Bioscience) and cloned by seeding a single cell into a 96-well plate to obtain AXL-high and AXL-low clones.

**Aldefluor assay.** ALDH activity was detected using the Aldefluor assay kit (StemCell Technologies, NC, USA) per the manufacturer's instructions. Separated sphere-derived cells were incubated with BODIPY-aminoacetaldehyde (BAAA) for 30 min at 37 °C. Cells that catalysed BAAA to BODIPY-aminoacetate were analysed by flow cytometry (BD FACSCanto II, BD Bioscience) to determine ALDH-positive cells. The baseline of fluorescence was determined using the ALDH inhibitor, N,N-diethylaminobenzaldehyde (DEAB)<sup>24</sup>. The percentage of ALDH-positive cells was analysed using FlowJo software (FlowJo, LLC, Ashland, OR, USA). The results are expressed as the means of three independent experiments  $\pm$  SD.

**Immunocytochemistry.** Tumour spheres were fixed with 4% paraformaldehyde containing 0.2% Triton X-100 for 20 min and then incubated with 25% BlockAce (KAC Co. Ltd, Tokyo Japan) for 10 min. Anti-ALDH1A1 antibody ( $\times$ 500 dilution in BlockAce) was used as the first antibody and AF488-labeled anti-mouse IgG was used as the second antibody. Stained spheres were observed with a fluorescent microscope (BIOREVO BZ-9000, Keyence, Osaka, Japan). The average fluorescent intensity was obtained by BZ-X Analysis Application (Keyence).

**Tumour xenograft experiments.** AXL-high or AXL-low clones ( $1 \times 10^6$  cells/100 µl saline) were injected at two sites of the subcutaneous flanks of six 5-week-old female SCID/Beige mice. Tumour growth was monitored for 35 days by taking caliper measurements of the tumour size. Tumour volume was calculated by the formula,  $\text{width}^2 \times \text{length}/2$ <sup>11</sup>. EGCG (100 mg/kg) was orally administered using an intubation tube, and 0.2% GTE solution

was additionally given as drinking water. EGCG + GTE was ingested from one day before injection of bulk H1299 cells until the end of the experiment. Tumour growth in the EGCG + GTE group was compared with that of the non-treated mice injected with bulk H1299 cells. All animal experiments were performed in accordance with the protocol approved by the International Animal Care and Use Committee of Saitama University (H30-A-1-12).

**Statistical analysis.** Statistical analyses were performed using one-way analysis of variance followed by Dunnett's test, while the Wilcoxon-Mann-Whitney test was used for analysing Young's modulus and the animal experiments. Each experiment was conducted independently at least three times, and values are expressed as the mean  $\pm$  SD.  $P < 0.05$  was considered statistically significant.

Received: 3 October 2019; Accepted: 22 January 2020;

Published online: 12 February 2020

## References

- Shimizu, M. *et al.* Green tea extracts for the prevention of metachronous colorectal adenomas: a pilot study. *Cancer Epidemiol. Biomarkers Prev.* **17**, 3020–3025, <https://doi.org/10.1158/1055-9965.EPI-08-0528> (2008).
- Shin, C. M. *et al.* Green tea extracts for the prevention of metachronous colorectal polyps among patients who underwent endoscopic removal of colorectal adenomas: A randomized clinical trial. *Clin. Nutr.* **37**, 452–458, <https://doi.org/10.1016/j.clnu.2017.01.014> (2018).
- Bettuzzi, S. *et al.* Chemoprevention of human prostate cancer by oral administration of green tea catechins in volunteers with high-grade prostate intraepithelial neoplasia: a preliminary report from a one-year proof-of-principle study. *Cancer Res.* **66**, 1234–1240, <https://doi.org/10.1158/0008-5472.CAN-05-1145> (2006).
- Fujiki, H. *et al.* Challenging the effectiveness of green tea in primary and tertiary cancer prevention. *J. Cancer Res. Clin. Oncol.* **138**, 1259–1270, <https://doi.org/10.1007/s00432-012-1250-y> (2012).
- Suganuma, M., Saha, A. & Fujiki, H. New cancer treatment strategy using combination of green tea catechins and anticancer drugs. *Cancer Sci.* **102**, 317–323, <https://doi.org/10.1111/j.1349-7006.2010.01805.x> (2011).
- Fujiki, H., Sueoka, E., Watanabe, T. & Suganuma, M. Synergistic enhancement of anticancer effects on numerous human cancer cell lines treated with the combination of EGCG, other green tea catechins, and anticancer compounds. *J. Cancer Res. Clin. Oncol.* **141**, 1511–1522, <https://doi.org/10.1007/s00432-014-1899-5> (2015).
- Fujiki, H., Sueoka, E., Rawangkan, A. & Suganuma, M. Human cancer stem cells are a target for cancer prevention using (–)-epigallocatechin gallate. *J. Cancer Res. Clin. Oncol.* **143**, 2401–2412, <https://doi.org/10.1007/s00432-017-2515-2> (2017).
- Cross, S. E., Jin, Y. S., Rao, J. & Gimzewski, J. K. Nanomechanical analysis of cells from cancer patients. *Nat. Nanotechnol.* **2**, 780–783, <https://doi.org/10.1038/nnano.2007.388> (2007).
- Cross, S. E., Jin, Y. S., Lu, Q. Y., Rao, J. & Gimzewski, J. K. Green tea extract selectively targets nanomechanics of live metastatic cancer cells. *Nanotechnol.* **22**, 215101, <https://doi.org/10.1088/0957-4484/22/21/215101> (2011).
- Takahashi, A. *et al.* Mechanism-based inhibition of cancer metastasis with (–)-epigallocatechin gallate. *Biochem. Biophys. Res. Commun.* **443**, 1–6, <https://doi.org/10.1016/j.bbrc.2013.10.094> (2014).
- Iida, K. *et al.* Cell softening in malignant progression of human lung cancer cells by activation of receptor tyrosine kinase AXL. *Sci. Rep.* **7**, 17770, <https://doi.org/10.1038/s41598-017-18120-4> (2017).
- Liu, E., Hjelle, B. & Bishop, J. M. Transforming genes in chronic myelogenous leukemia. *Proc. Natl Acad. Sci. USA* **85**, 1952–1956, <https://doi.org/10.1073/pnas.85.6.1952> (1988).
- O'Bryan, J. P. *et al.* axl, a transforming gene isolated from primary human myeloid leukemia cells, encodes a novel receptor tyrosine kinase. *Mol. Cell Biol.* **11**, 5016–5031, <https://doi.org/10.1128/mcb.11.10.5016> (1991).
- Graham, D. K., DeRyckere, D., Davies, K. D. & Earp, H. S. The TAM family: phosphatidylerine sensing receptor tyrosine kinases gone awry in cancer. *Nat. Rev. Cancer* **14**, 769–785, <https://doi.org/10.1038/nrc3847> (2014).
- Seike, M. *et al.* AXL and GAS6 co-expression in lung adenocarcinoma as a prognostic classifier. *Oncol. Rep.* **37**, 3261–3269, <https://doi.org/10.3892/or.2017.5594> (2017).
- Zhang, Z. *et al.* Activation of the AXL kinase causes resistance to EGFR-targeted therapy in lung cancer. *Nat. Genet.* **44**, 852–860, <https://doi.org/10.1038/ng.2330> (2012).
- Gay, C. M., Balaji, K. & Byers, L. A. Giving AXL the axe: targeting AXL in human malignancy. *Br. J. Cancer* **116**, 415–423, <https://doi.org/10.1038/bjc.2016.428> (2017).
- Asiedu, M. K. *et al.* AXL induces epithelial-to-mesenchymal transition and regulates the function of breast cancer stem cells. *Oncogene* **33**, 1316–1324, <https://doi.org/10.1038/onc.2013.57> (2014).
- Jin, Y. *et al.* Gas6/AXL signaling regulates self-renewal of chronic myelogenous leukemia stem cells by stabilizing  $\beta$ -catenin. *Clin. Cancer Res.* **23**, 2842–2855, <https://doi.org/10.1158/1078-0432.CCR-16-1298> (2017).
- Cheng, P. *et al.* Kinome-wide shRNA screen identifies the receptor tyrosine kinase AXL as a key regulator for mesenchymal glioblastoma stem-like cells. *Stem Cell Rep.* **4**, 899–913, <https://doi.org/10.1016/j.stemcr.2015.03.005> (2015).
- Suganuma, M. *et al.* Biophysical approach to mechanisms of cancer prevention and treatment with green tea catechins. *Molecules* **21**, <https://doi.org/10.3390/molecules21111566> (2016).
- Watanabe, T. *et al.* Higher cell stiffness indicating lower metastatic potential in B16 melanoma cell variants and in (–)-epigallocatechin gallate-treated cells. *J. Cancer Res. Clin. Oncol.* **138**, 859–866, <https://doi.org/10.1007/s00432-012-1159-5> (2012).
- Haghighparast, S. M., Kihara, T. & Miyake, J. Distinct mechanical behavior of HEK293 cells in adherent and suspended states. *PeerJ* **3**, e1131, <https://doi.org/10.7717/peerj.1131> (2015).
- Sullivan, J. P. *et al.* Aldehyde dehydrogenase activity selects for lung adenocarcinoma stem cells dependent on notch signaling. *Cancer Res.* **70**, 9937–9948, <https://doi.org/10.1158/0008-5472.CAN-10-0881> (2010).
- Toden, S., Tran, H. M., Tovar-Camargo, O. A., Okugawa, Y. & Goel, A. Epigallocatechin-3-gallate targets cancer stem-like cells and enhances 5-fluorouracil chemosensitivity in colorectal cancer. *Oncotarget* **7**, 16158–16171, <https://doi.org/10.18632/oncotarget.7567> (2016).
- Sun, J. *et al.* Biomechanical profile of cancer stem-like cells derived from MHCC97H cell lines. *J. Biomech.* **49**, 45–52, <https://doi.org/10.1016/j.jbiomech.2015.11.007> (2016).
- Chen, W. *et al.* Biophysical phenotyping and modulation of ALDH+ inflammatory breast cancer stem-like cells. *Small* **15**, e1802891, <https://doi.org/10.1002/sml.201802891> (2019).
- Sun, J. *et al.* Salinomycin attenuates liver cancer stem cell motility by enhancing cell stiffness and increasing F-actin formation via the FAK-ERK1/2 signalling pathway. *Toxicol.* **384**, 1–10, <https://doi.org/10.1016/j.tox.2017.04.006> (2017).
- Gupta, P. B. *et al.* Identification of selective inhibitors of cancer stem cells by high-throughput screening. *Cell* **138**, 645–659, <https://doi.org/10.1016/j.cell.2009.06.034> (2009).

30. Kashyap, V. *et al.* Regulation of stem cell pluripotency and differentiation involves a mutual regulatory circuit of the NANOG, OCT4, and SOX2 pluripotency transcription factors with polycomb repressive complexes and stem cell microRNAs. *Stem Cell Dev.* **18**, 1093–1108, <https://doi.org/10.1089/scd.2009.0113> (2009).
31. Vassalli, G. *et al.* Aldehyde dehydrogenases: Not just markers, but functional regulators of stem cells. *Stem Cell Int.* **2019**, <https://doi.org/10.1155/2019/3904645> (2019).
32. Luanpitpong, S. *et al.* Slug is required for SOX9 stabilization and functions to promote cancer stem cells and metastasis in human lung carcinoma. *Oncogene* **35**, 2824–2833, <https://doi.org/10.1038/onc.2015.351> (2016).
33. Antony, J. *et al.* The GAS6-AXL signaling network is a mesenchymal (Mes) molecular subtype-specific therapeutic target for ovarian cancer. *Sci. Signal.* **9**, ra97, <https://doi.org/10.1126/scisignal.aaf8175> (2016).
34. Gujral, T. S. *et al.* Profiling phospho-signaling networks in breast cancer using reverse-phase protein arrays. *Oncogene* **32**, 3470–3476, <https://doi.org/10.1038/onc.2012.378> (2013).
35. Wu, X. *et al.* AXL-GAS6 expression can predict for adverse prognosis in non-small cell lung cancer with brain metastases. *J. Cancer Res. Clin. Oncol.* **143**, 1947–1957, <https://doi.org/10.1007/s00432-017-2408-4> (2017).
36. Matsuzaki, T. *et al.* Adsorption of galloyl catechin aggregates significantly modulates membrane mechanics in the absence of biochemical cues. *Phys. Chem. Chem Phys* **19**, 19937–19947, <https://doi.org/10.1039/c7cp02771k> (2017).
37. Kim, K. C. & Lee, C. Reversal of Cisplatin resistance by epigallocatechin gallate is mediated by downregulation of axl and tyro 3 expression in human lung cancer cells. *Korean J. Physiol. Pharmacol.* **18**, 61–66, <https://doi.org/10.4196/kjpp.2014.18.1.61> (2014).
38. Wei, M., Korotkov, K. V. & Blackburn, J. S. Targeting phosphatases of regenerating liver (PRLs) in cancer. *Pharmacol. Ther.* **190**, 128–138, <https://doi.org/10.1016/j.pharmthera.2018.05.014> (2018).
39. Johnson, S., Chen, H. & Lo, P. K. *In vitro* tumorsphere formation assays. *Bio. Protoc* **3** (2013).
40. Rawangkan, A. *et al.* Green tea catechin is an alternative immune checkpoint inhibitor that inhibits PD-L1 expression and lung tumor growth. *Molecules* **23**, 2071, <https://doi.org/10.3390/molecules23082071> (2018).

## Acknowledgements

We thank Dr. Takanori Kihara at the Faculty of Environmental Engineering, The University of Kitakyushu, and Dr. Kouichi Tachibana, National Institute of Advanced Industrial Science and Technology, for assisting with the BAM coating; Dr. Atsushi Takahashi, Saitama Tea Institute for providing GTE; Dr. Tomoyuki Ohba, URA office, Saitama University, for useful discussions; and Kaori Suzuki, Miki Kanno, and Ikuko Shiotani at Saitama University for their technical assistance. We also thank Prof. Hirota Fujiki at the Faculty of Medicine, Saga University, for his warm encouragement and Dr. Tatsuro Watanabe at the Faculty of Medicine, Saga University for his fruitful discussions. This work was supported by the Smoking Research Fund, the Urakami Foundation, and the Takeda Science Foundation. Finally, we thank H. Nikki March, PhD, from Edanz Group (www.edanzediting.com/ac) for editing a draft of this manuscript.

## Author contributions

K.N. and M.S. conceived the experiments, K.N., P.W., S.Y., M.S., A.R., R.S. and K.I. conducted the experiments, K.N., P.W., S.Y. and M.S. analysed the results, and K.N. and M.S. wrote the manuscript. All authors reviewed the manuscript.

## Competing interests

The authors declare no competing interests.

## Additional information

**Supplementary information** is available for this paper at <https://doi.org/10.1038/s41598-020-59281-z>.

**Correspondence** and requests for materials should be addressed to M.S.

**Reprints and permissions information** is available at [www.nature.com/reprints](http://www.nature.com/reprints).

**Publisher's note** Springer Nature remains neutral with regard to jurisdictional claims in published maps and institutional affiliations.



**Open Access** This article is licensed under a Creative Commons Attribution 4.0 International License, which permits use, sharing, adaptation, distribution and reproduction in any medium or format, as long as you give appropriate credit to the original author(s) and the source, provide a link to the Creative Commons license, and indicate if changes were made. The images or other third party material in this article are included in the article's Creative Commons license, unless indicated otherwise in a credit line to the material. If material is not included in the article's Creative Commons license and your intended use is not permitted by statutory regulation or exceeds the permitted use, you will need to obtain permission directly from the copyright holder. To view a copy of this license, visit <http://creativecommons.org/licenses/by/4.0/>.

© The Author(s) 2020